

Spatial correlation for horizontal and vertical components of acceleration from northern Iran seismic events

Alireza Garakaninezhad · Morteza Bastami ·
Mohammad Reza Soghrat

Received: 18 February 2017 / Accepted: 6 July 2017 / Published online: 19 July 2017
© Springer Science+Business Media B.V. 2017

Abstract The evaluation of seismic risk of spatially distributed systems requires the spatial correlation model for ground motion intensity measures. This study investigates the spatial correlation of four earthquakes recorded in northern Iran. The intra-event spatial correlation for both horizontal and vertical components of spectral acceleration at eight periods in the range of 0.0–3.0 s is estimated using geostatistical tools. An exponential form is chosen to fit experimental semivariograms, and the correlation ranges of spectral accelerations as a function of period are derived. The results show similar trend of correlation ranges for both components. It should be mentioned that the ranges for the vertical component, in general, are higher than those observed for the horizontal one. For both components, the correlation ranges as a function of period are divided into three segments. The first and the third one are increasing while the second one is decreasing with increasing period.

Keywords Lifelines · Spatial correlation · Risk assessment · Spectral accelerations

A. Garakaninezhad · M. Bastami (✉) · M. R. Soghrat
International Institute of Earthquake Engineering and Seismology (IIEES), No. 26, Arghavan St., North Dibajee, Farmanieh, P.O. Box: 19395, Tehran /3913, Iran
e-mail: m.bastami@iiees.ac.ir

A. Garakaninezhad
e-mail: a.garakani@iiees.ac.ir

M. R. Soghrat
e-mail: m.soghrat@iiees.ac.ir

1 Introduction

Estimating spatial correlation ground motion intensity measures (IMs) over a region is necessary to assess seismic risk of lifeline networks such as transportation, electrical and gas networks, telecommunications, and water supply. This requires to consider the correlation between ground motion IMs during different earthquakes (inter-event correlation) and at different sites (intra-event correlation). Several researchers investigated the effects of spatial correlation of ground motion IMs on loss assessment of spatially distributed systems. It is shown that ignoring or underestimating the spatial correlation may overestimate frequent losses and underestimate rare ones (Bastami 2007; Bazzurro and Luco 2007; Lee and Kiremidjian 2007; Park et al. 2007). Some studies used only a specific earthquake scenario (Crowley et al. 2008; Goda and Atkinson 2009; Lee et al. 2004; Lee and Kiremidjian 2007; Molas et al. 2006; Sokolov and Wenzel 2011b) which in general analyzed the intra-event correlation effects. Multiple earthquakes were investigated by Goda and Hong (2008a), Goda and Hong (2009), McVerry et al. (2004), Park et al. (2007), Sokolov and Wenzel (2011a), and Wesson and Perkins (2001) who in general considered both inter- and intra-event correlations. Bommer and Crowley (2006) and Crowley and Bommer (2006) introduced two procedures to estimate loss exceedance curve. The first method is based on independent probabilistic seismic hazard assessment, and the other has used a scenario-based Monte Carlo simulation approach based on the seismicity model.

The loss calculation approaches are based on ground motion IMs. In general, ground motion IMs, such as peak ground acceleration (PGA), peak ground velocity (PGV), and spectral accelerations (SAs), can be obtained using ground motion prediction equations (GMPEs). These equations are presented as a function of earthquake magnitude, source-to-site distance, faulting mechanism, local site conditions such as V_{s30} (time-averaged shear wave velocity in the top 30 m), and other parameters. GMPEs can account for the effects of spatial variations, and to do this, the database used and the regression method are very important. Partially nonergodic GMPE models developed by Gianniotis et al. (2014), Kotha et al. (2016), Sedaghati and Pezeshk (2017), and Stafford (2014) can account for spatial variability for distinct regions. In addition, Landwehr et al. (2016) presented a fully nonergodic ground motion model for California records with coefficients that vary continuously on a spatial scale. However, most of old GMPEs cannot model spatial correlation of IMs at different sites because of their regression methods or database used.

In the literature, several spatial correlation models for different IMs have been introduced. Boore et al. (2003) used the 1994 Northridge earthquake observations to compute spatial correlation model of PGA. Wang and Takada (2005) computed spatial correlation of PGV using several earthquakes in Japan and the 1999 Chi-Chi earthquake. Goda and Hong (2008b) and Jayaram and Baker (2009) computed spatial correlation models based on the 1999 Chi-Chi earthquake and some well-recorded earthquakes in California, and Hong et al. (2009) used only some earthquakes in California. In these studies, the models were proposed using well-recorded individual earthquakes, such as the 1994 Northridge earthquake. In fact, in these studies, the correlation ranges of each earthquake were investigated separately; then, a model based on obtained ranges was proposed. However, in the other approach, spatial correlations were investigated based on gathering the data from a group of earthquakes. Goda and Atkinson (2010) proposed models based on comprehensive databases accumulated in Japan. Esposito and Iervolino (2011, 2012) used the Italian accelerometric archive and the European strong-motion database and Pavel and Vacareanu (2016) used Vrancea (Romania) intermediate-depth earthquakes. The models in above-mentioned studies investigated the spatial correlation of single IMs at different sites, and in most cases, the

horizontal component is considered. The spatial cross correlation of vector IMs was presented by some researchers. For example, Loth and Baker (2013) and Du and Wang (2013) investigated the spatial cross correlation of SAs at multiple periods. In other study, Wang and Du (2013) proposed models for two sets of vector IMs: the first set (PGA, PGV, and I_a) and the second set (SAs at multiple periods) considering the effects of regional site conditions. The results reported by these studies show different rates of decay of correlation with site-to-site separation distance. Some studies investigated the effects of local site conditions on spatial correlation of IMs (Du and Wang 2013; Jayaram and Baker 2009; Sokolov and Wenzel 2013; Sokolov et al. 2012; Wang and Du 2013). These studies reported that spatial correlation of IMs tends to be stronger if the regional site conditions are more homogeneous. The spatial homogeneity of a region can be presented using the spatial correlation of V_{s30} . The region whose range of V_{s30} is larger shows a more homogeneous site condition.

Spatial correlation models of IMs have not been estimated for the Iranian plateau so far. However, it has experienced destructive earthquakes since ancient times and has a long history of seismicity (Ambraseys and Melville 2005; Berberian and Yeats 1999). Therefore, the spatial correlation models are required to accurately perform seismic hazard analysis. In addition, aforementioned models were proposed for horizontal component of earthquake, although the importance of vertical component of earthquake in inflicting damage has been shown in some earthquakes such as 1995 Kobe, 1999 Chi-Chi, and 2005 Bam (Elgamal and He 2004; Papazoglou and Elnashai 1996; Zahrai and Heidarzadeh 2007). In particular, for a transportation network including bridges in which the vertical component of earthquake is significant, the derived correlation ranges for vertical component can be useful. Esposito et al. (2010) analyzed spatial correlation of vertical component PGA based on European data; however, a model for vertical SAs has not been proposed so far.

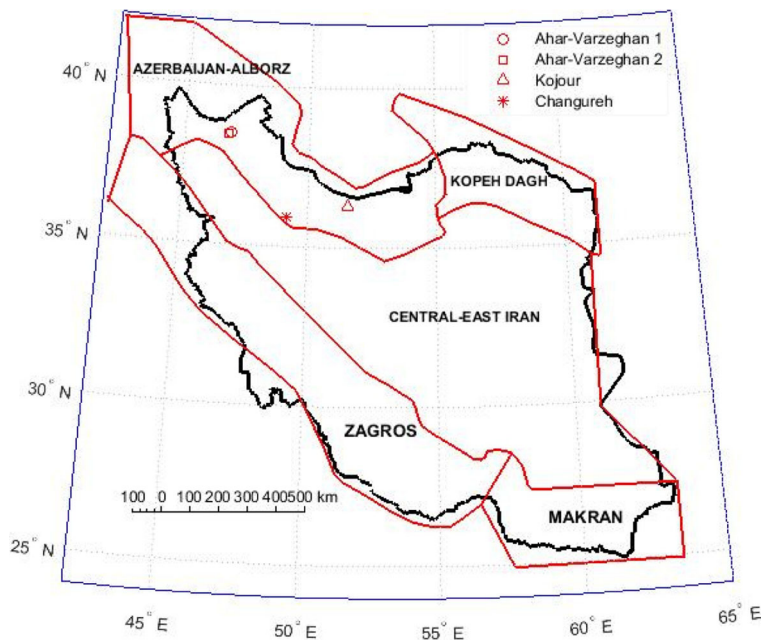
In this study, spatial correlation models for horizontal and vertical spectral acceleration based on four earthquakes in northern Iran were proposed. Four earthquake events with considerable number of records were selected. These earthquakes were located in the northern Iranian plateau. The residual for each IM was computed using the GMPE developed by Soghrat and Ziyaeifar (2016) [SZ-16] which was derived based on northern Iranian plateau earthquake records. The

computation of spatial correlation was performed using semivariogram as geostatistical tools. Then, the ranges of spatial correlation were presented for eight periods, ranging from 0.0 to 3.0 s. Since computing empirical variogram needs a relatively large number of data which are not available for individual earthquakes in the selected datasets, data from multiple earthquakes were pooled to estimate the correlations. This approach has been used by Esposito and Iervolino (2011, 2012). Finally, based on the results, models for spatial correlation ranges as a function of structural period were proposed. The obtained ranges are necessary to quantify regional seismic risk.

2 Database of ground motions

The Iranian plateau as a large prone zone is divided into five tectonic regions (Azerbaijan-Alborz, Kopeh Dagh, central-east Iran, Makran, and Zagros) classified by Mirzaei et al. (1998), as shown in Fig. 1. The earthquakes considered in this study were located in Azerbaijan-Alborz region in northern Iran. The ground motion model proposed by Soghrat and Ziyaeifar (2016) was developed for Azerbaijan-Alborz and Kopeh Dagh regions. Figure 2 shows the map of stations for four considered earthquakes: 2002 Changureh, 2004 Kojour, double events of 2012 Ahar-Varzeghan.

Fig. 1 Tectonic regions in the Iranian plateau (Mirzaei et al. 1998) and the considered earthquakes



Additional information about these events is listed in Table 1. The stations with available site class were considered in this study. These classifications are based on the Standard 2800 (Iranian Code of Practice for Seismic Resistant design of Building). Sites are classified into four groups in term of V_{s30} (I- $V_{s30} > 750$ m/s, II- $375 < V_{s30} < 750$ m/s, III- $175 < V_{s30} < 375$ m/s, and IV- $V_{s30} < 175$ m/s). Figure 3 shows the magnitude-distance distribution of events considered.

3 Investigation of spatial correlations of IM residuals

The theoretical background of computing spatial correlation is discussed in several references (Du and Wang 2013; Jayaram and Baker 2008; Sokolov and Wenzel 2013). Hence, in this section, it will be reviewed briefly. In general, a ground motion IM recorded at site i , triggered by earthquake j , can be estimated by GMPEs as follows

$$\ln(Y_{ij}) = \ln\bar{Y}_{ij}(M, R, \theta) + \varepsilon_{ij} + \eta_j \tag{1}$$

where $\bar{Y}_{ij}(M, R, \theta)$ denotes the predicted mean value of ground motion intensity, M denotes the earthquake magnitude, R is the site-to-source distance, θ shows the other parameters, such as local site conditions and faulting mechanism. ε_{ij} and η_j indicate the intra- and inter-event residuals, respectively. These terms are assumed to be

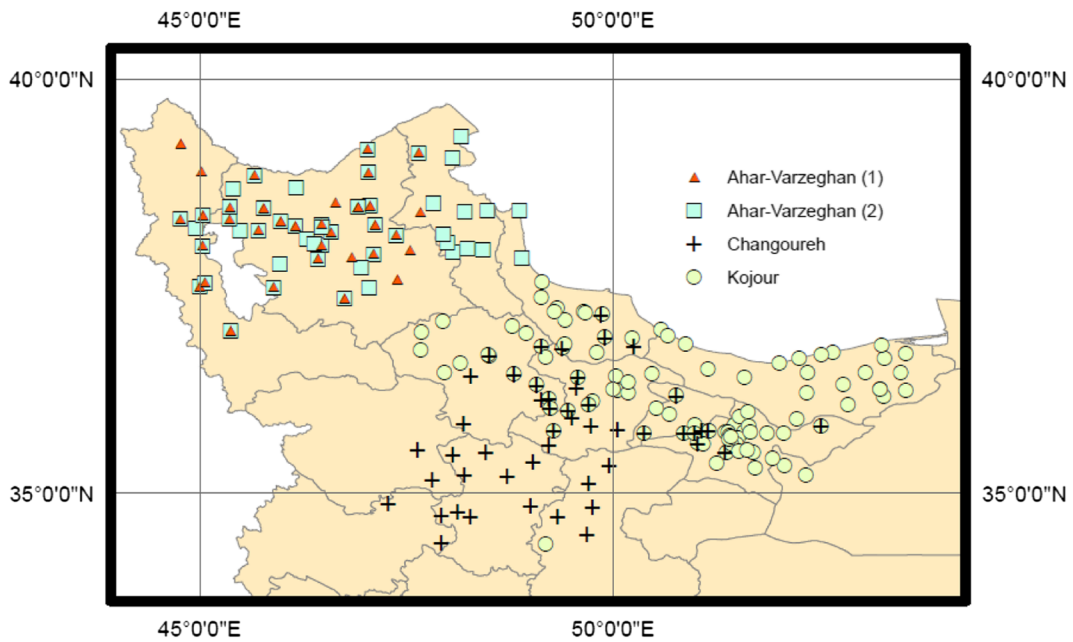


Fig. 2 Location of stations of four considered earthquakes

normal variables with zero mean and standard deviations of σ_{ij} and τ_j , respectively (Jayaram and Baker 2008).

The predicted values of IMs for both horizontal and vertical component were computed at eight different periods using the SZ-16 model. The horizontal component defined in SZ-16 is the geometric mean of N-S and E-W. This model is proposed in two forms based on either the value of V_{s30} or site class. Because the V_{s30} values for all stations were not available, the second form of SZ-16 model was used. The SZ-16 model is calibrated in this study because we used more records than the database of Soghrat and Ziyaeifar (2016). The observed bias for PGA and SA ($T = 1.0$ s) by using the SZ-16 model is shown in Fig. 4. The estimated residuals are corrected and the bias is removed. This can be performed as follows (Du and Wang 2013)

$$\varepsilon_{ij}^{corr} = \varepsilon_{ij} - (\alpha_1 + \alpha_2 \ln(R_{rup})) \tag{2}$$

in which α_1 and α_2 denote the coefficients computed by linear regression. In order to accurately compute the intra-event spatial correlations, the residuals can be normalized as follows

$$\hat{\varepsilon}_{ij} = \frac{\varepsilon_{ij}^{corr}}{\sigma_{ij}} \cong \frac{\ln(Y_{ij}) - \ln \bar{Y}_{ij}(M, R, \theta) - (\alpha_1 + \alpha_2 \ln(R_{rup}))}{\sigma_{ij}} \tag{3}$$

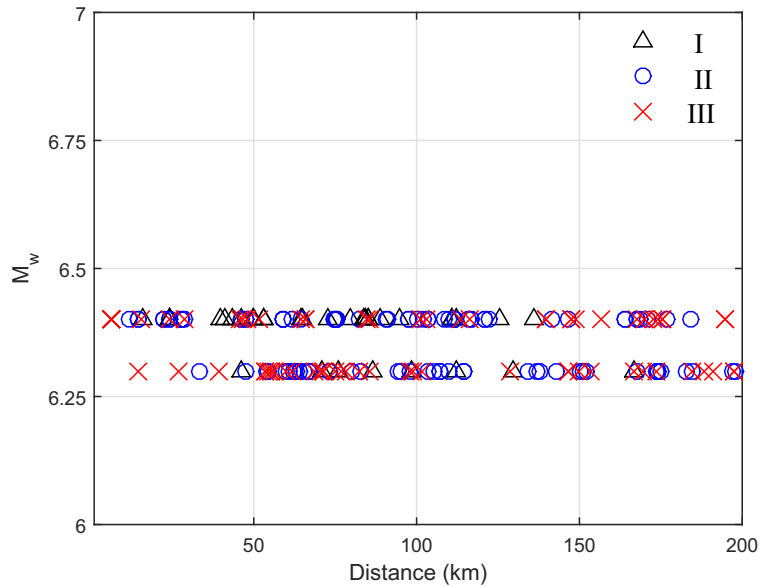
where $\hat{\varepsilon}_{ij}$ indicates the normalized corrected intra-event residuals. The spatial correlation of these residuals can be investigated using semivariogram which is widely used in geostatistics. The semivariogram, $\gamma(\mathbf{h})$, identifies the spatial decorrelation or dissimilarity between data separated by a vector \mathbf{h} (Cressie 1993). Under the second-order stationary assumption, the semivariogram function can be written as follows

$$\gamma(\mathbf{h}) = \frac{1}{2} E \left[(Z_{u_i} - Z_{u_i+\mathbf{h}})^2 \right] \tag{4}$$

Table 1 Earthquake events used in this study

Earthquake name	Date	Latitude	Longitude	Magnitude (Mw)	Depth (km)	Fault mechanism	Number of records
Changureh	06/22/2002	35.67	48.93	6.4	10.0	Reverse	47
Kojour	05/28/2004	36.281	51.582	6.3	17.0	Reverse	92
Ahar-Varzeghan (1)	08/11/2012	38.31	46.80	6.4	7.0	Strike slip	35
Ahar-Varzeghan (2)	08/11/2012	38.394	46.814	6.4	19.2	Reverse	53

Fig. 3 Distribution of moment magnitude-distance and corresponding soil classes



where Z_{u_i+h} and Z_{u_i} are the random variables separated by the separation vector \mathbf{h} and $E[\]$ denotes the expectation. In this study, the random variable is referred to the normalized corrected intra-event residual, $\hat{\epsilon}_{ij}$. The second-order stationarity of a random field implies that the mean value of the random variable is constant over the entire domain and the semivariogram values depend only on the separation vector \mathbf{h} and not on actual location \mathbf{u} . In addition, the stationary semivariogram is isotropic if it is independent of the direction; therefore, the vector \mathbf{h} in Eq. (4) can be replaced by its norm $\|\mathbf{h}\|$.

The experimental semivariogram for second-order random field can be computed as follows

$$\hat{\gamma}(h) = \frac{1}{2N(h)} \sum_{i=1}^{N(h)} [(Z_{u_i} - Z_{u_i+h})^2] \tag{5}$$

in which $N(h)$ denotes the number of pairs separated by h and $\gamma(h)$ denotes the empirical semivariogram (Cressie 1993). Several parametric functions have been proposed to approximate the empirical semivariogram values. Three basic forms can be considered: Gaussian,

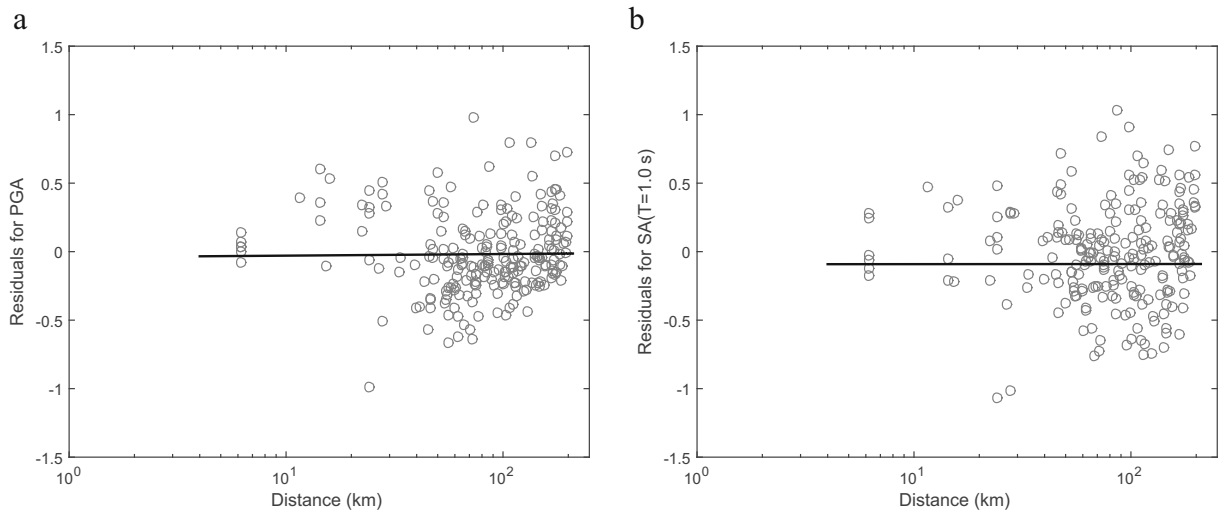


Fig. 4 Distribution of intra-event residuals for horizontal acceleration component **a** PGA, **b** SA (at $T = 1.0$ s)

Spherical, and Exponential models (Cressie 1993). The exponential model which is widely used in the literature is applied to fit a model. This model can be written as

$$\gamma(h) = a \left[1 - e^{-\frac{3h}{b}} \right] + c \quad (6)$$

where a is the sill of the semivariogram and equals the variance of empirical data and b shows the range of the semivariogram which is defined as the separation distance when the semivariogram reaches 0.95 times the sill, c denotes the nugget that is defined the semivariogram value when h tends to zero (Cressie 1993).

4 Spatial correlation models

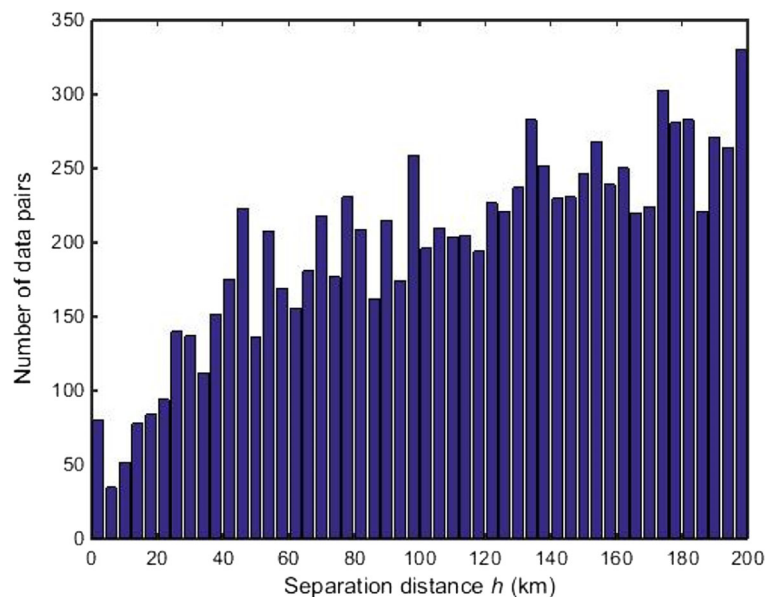
This section discusses the ranges of semivariograms for both horizontal and vertical components evaluated using considered earthquakes. To estimate semivariogram values, it is important to have at least 30 pairs in each distance bin (Cressie 1993; Journel and Huijbregts 1978). Therefore, a bin width of 4 km and the maximum site-to-source distance of 200 km are considered. Figure 5 shows the number of pairs in each bin as a function of separation distance. The exponential model was selected to fit experimental values because this model is widely used by other researchers (e.g., Esposito and Iervolino 2011; Esposito and Iervolino 2012; Jayaram and Baker 2009). It is assumed that the

model includes the nugget effect. Therefore, in eq. 6, the range b and the sill a are parameters which are required to estimate. There are several methods to estimate this parameter, such as the least square fit, weighted least square (WLS) fit, and the manual fitting method (Du and Wang 2013; Jayaram and Baker 2009; Wang and Du 2013). In WLS, the weight is selected $\frac{1}{h_k}$, where h_k denotes the center of each bin and this leads to better approximation for the experimental values in close separation distance bins. WLS fitting approach is also applied by Wang and Du (2013). Since the correlations of the large separation distances are low, hence, these correlations have no significant effect on joint distributions of ground motion IMs. In this study, both manual and WLS fitting approaches are performed to estimate the model parameters. The comparison of these approaches shows that the predicted values using WLS for short separation distances, less than 50 km, are more accurate. Therefore, in this study, WLS is used to estimate the parameters of the exponential model.

Figure 6 shows the experimental semivariograms and corresponding fitted models for horizontal SAs at eight periods ranging between 0.0 and 3.0 s. For each period, the exponential model is built using WLS approach. The results show that the range of SA at $T = 3$ s is the largest and the correlation decays at this period slower than the others. The minimum range is obtained for $T = 1$ s.

Figure 7 shows the experimental semivariogram values for vertical component of SAs and fitted models

Fig. 5 The number of data pairs as a function of site-to-site separation distance



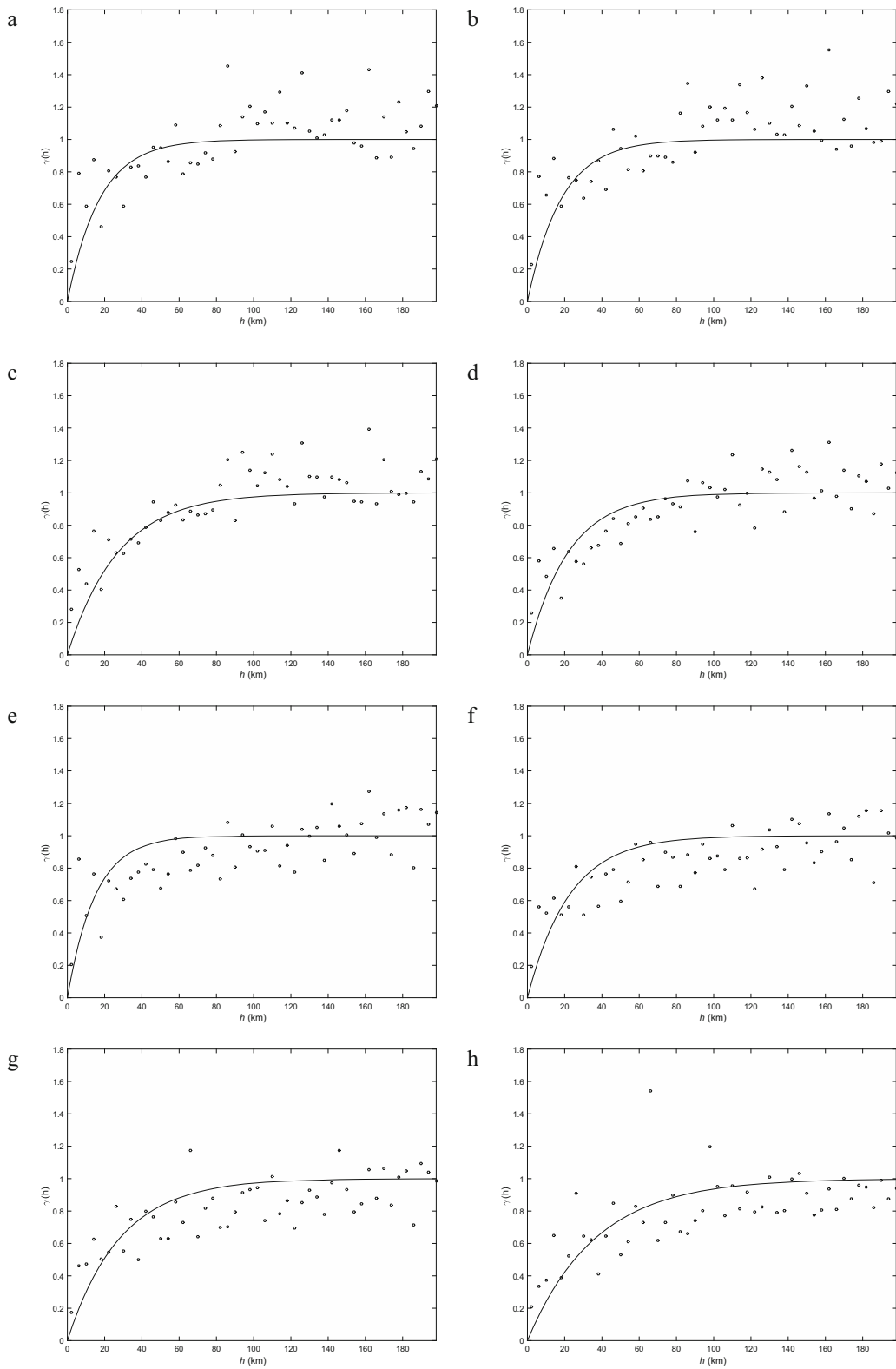


Fig. 6 Experimental semivariogram values and exponential fitted model for horizontal acceleration components; **a** PGA, **b** SA ($T=0.2$ s), **c** SA ($T=0.5$ s), **d** SA ($T=0.7$ s), **e** SA ($T=1.0$ s), **f** SA ($T=1.5$ s), **g** SA ($T=2.0$ s), **h** SA ($T=3.0$ s)

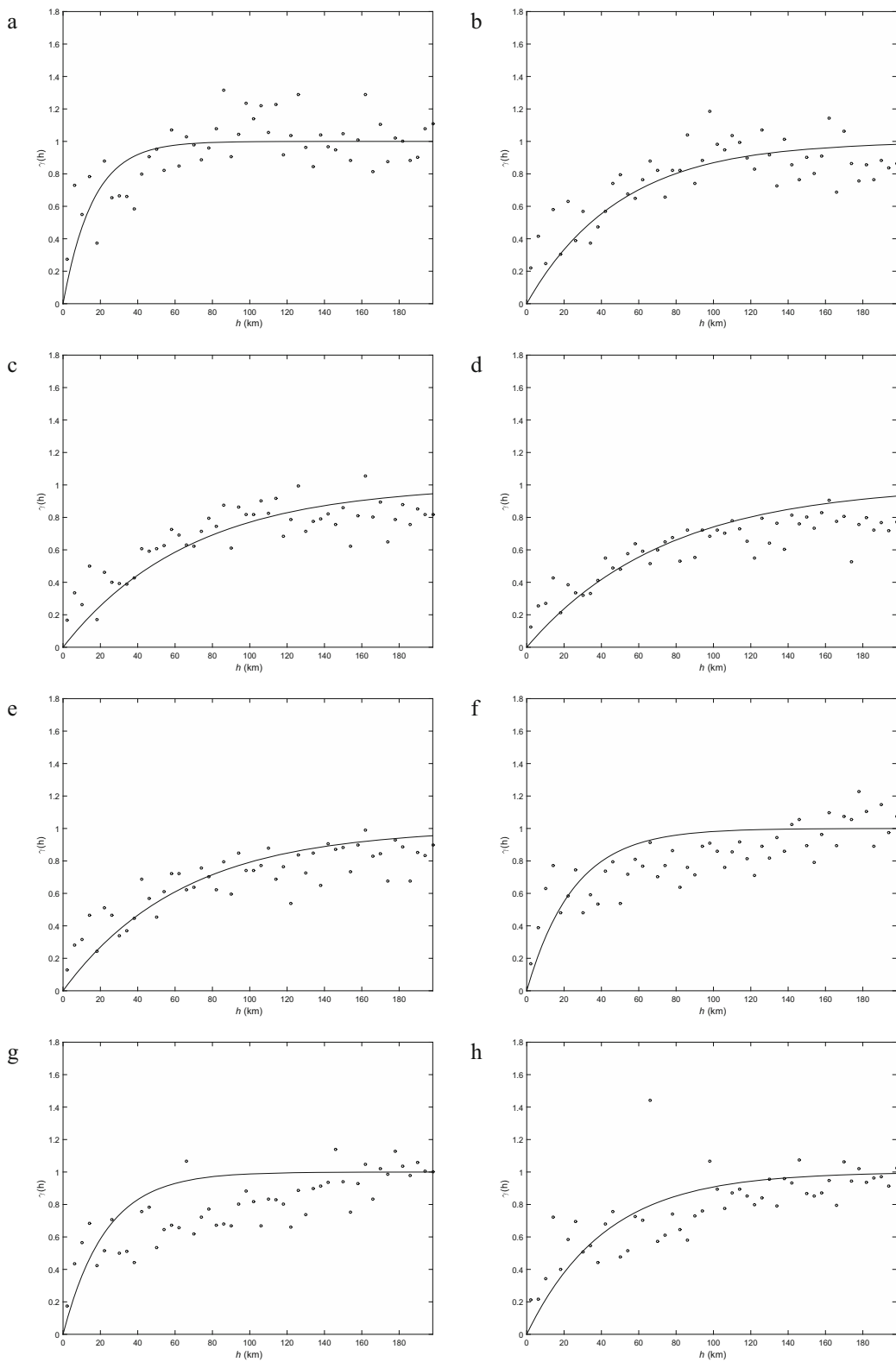


Fig. 7 Experimental semivariogram values and exponential fitted model for vertical acceleration components; **a** PGA, **b** SA ($T=0.2$ s), **c** SA ($T=0.5$ s), **d** SA ($T=0.7$ s), **e** SA ($T=1.0$ s), **f** SA ($T=1.5$ s), **g** SA ($T=2.0$ s), **h** SA ($T=3.0$ s)

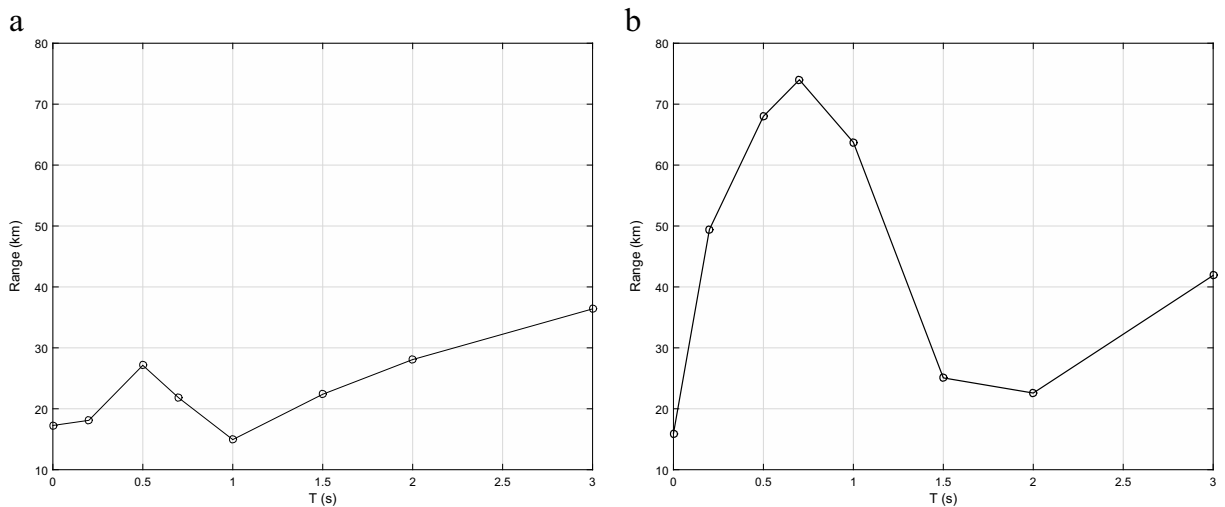


Fig. 8 Correlation ranges: **a** horizontal and **b** vertical spectral acceleration components as a function of period

for eight periods. As it can be seen, in general, the correlations decay slower in comparison with the horizontal components, especially in periods between $T = 0.5$ s and $T = 1$ s. Figure 8a indicates the estimated ranges as a function of spectral periods. It can be seen from this figure that the estimated correlation range tends to increase with period, except for short periods ($T < 1.0$ s). This behavior observed in past studies of

ground motion coherency, which can be considered as a measure of similarity in two spatially separated ground motion time histories (Zerva and Zervas 2002). The trend of correlation ranges can be approximated by three segments: $0 \leq T \leq 0.5$ s, $0.5 \leq T \leq 1$ s, and $T \geq 1$ s. The first segment is increasing up to $T = 0.5$ s which is in contrast with the other studies. However, the second and third segments are similar to the others. The second

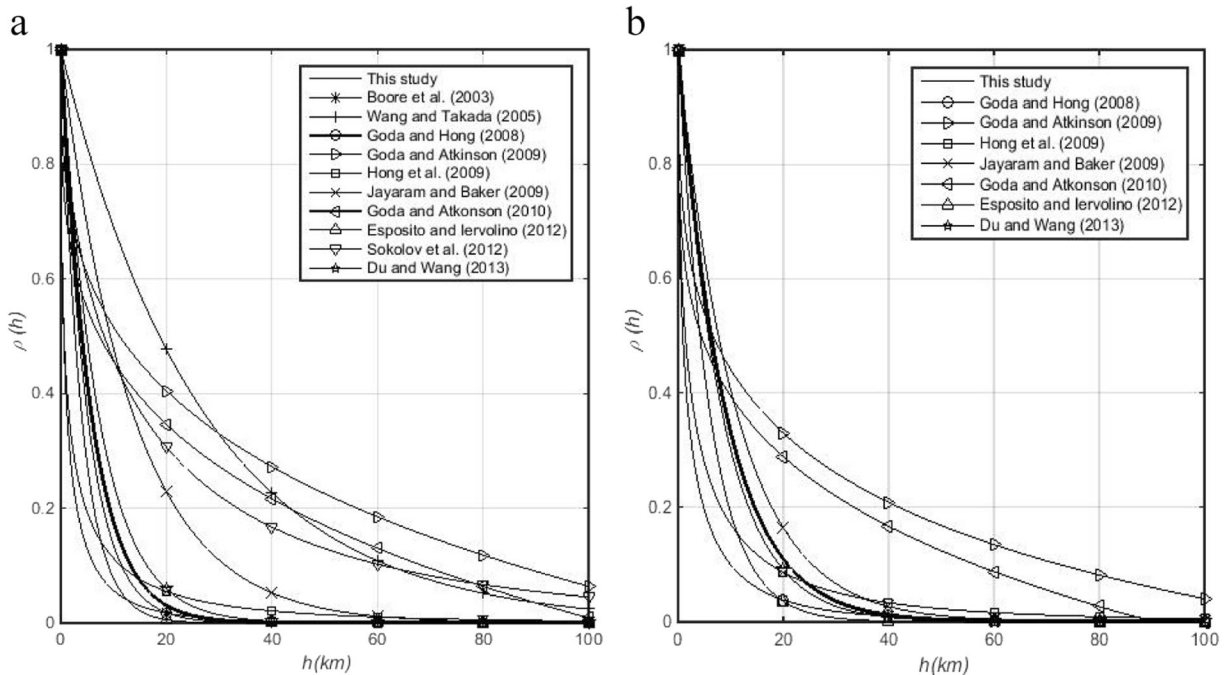


Fig. 9 Comparison of existing correlation models for horizontal acceleration component, **a** PGA and **b** SA ($T = 0.5$ s)

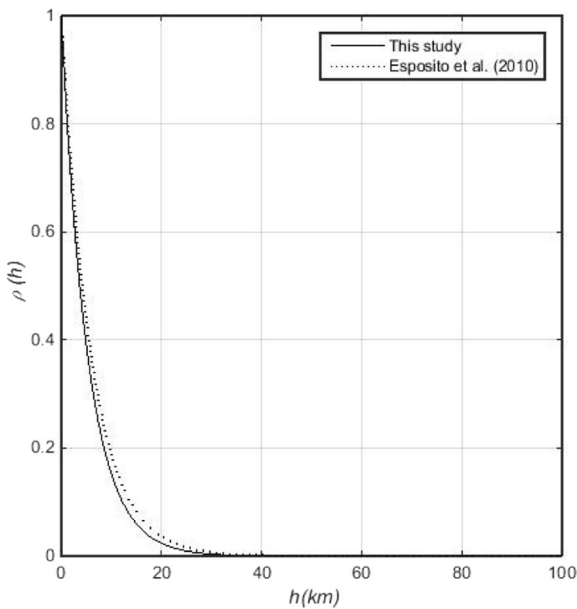


Fig. 10 Comparison of correlation model for vertical PGA obtained from this study with the model proposed by Esposito et al. (2010)

decreasing segment was also observed by Jayaram and Baker (2008), Jayaram and Baker (2009), and Zerva and Zervas (2002) for sites with similar geological conditions. The ranges in this segment decrease up to $T = 1$ s. In the third segment, the trend is increasing as seen in the model of Jayaram and Baker (2009). In this segment, the rate of increasing range is larger than the models proposed by Jayaram and Baker (2009) and Du and Wang (2013), however, is consistent with the predicted model presented by Esposito and Iervolino (2012). However, the ranges estimated in the present study for long period are smaller in comparison with the results in previous studies.

Figure 8b shows the ranges of vertical component of SAs as a function of periods. The trend of ranges for vertical is similar to horizontal and can be divided into three segments. In the first segment, ranges increase up to $T = 0.7$ s; then, ranges have the decreasing trend up to $T = 2$ s. In fact, in this case, the decreasing part is larger than that of horizontal SAs. The ranges increase in the third segment. It can be seen from Fig. 8b that the correlation range tends to decrease with period in 0.7 s, 2.0 s. The decreasing trend of correlation range in long period is reported by Abrahamson et al. (1991). They studied the vertical ground motion coherency and observed that, at certain distances, the lagged coherency attained lower values at lower frequencies.

Finally, the ranges obtained in this study are compared with those of proposed by the other studies. Figure 9 compares the intra-event correlation of horizontal PGA and SA ($T = 0.5$ s) obtained from the proposed model in this study for northern Iranian earthquakes with the results from models proposed by the other researchers in the literature. Figure 9a shows that the correlation ranges of PGA residuals of this study are similar to those of the models proposed by Boore et al. (2003), Goda and Hong (2008b), Esposito and Iervolino (2012), and Du and Wang (2013). For distance less than 20 km, the model proposed by Boore et al. (2003) gives the most correlation. The comparison of empirical correlation of SA ($T = 0.5$ s) from the proposed model with that of existing models, Fig. 9b, indicates that the model proposed by Du and Wang (2013) gives more correlation.

Figure 10 compares the empirical correlation of vertical PGA from this study with that of the model proposed by Esposito et al. (2010). This figure shows that the decays of these studies are similar.

5 Conclusion

This study proposed the spatial correlation models based on four earthquakes in northern Iran. The spatial correlation for horizontal and vertical components of spectral acceleration at eight periods was investigated using geostatistical tools, which are widely applied in the other similar studies. Because the stations are located in a relatively large region, records from different events were pooled to derive the models.

Based on the results presented in this study, an exponential form was chosen for the proposed models. Results show similar trend of correlation ranges for both horizontal and vertical components. However, the ranges for vertical components of SAs are larger than the horizontal ones. These ranges as a function of period can be divided into three segments. The first and the third one are increasing while the second is decreasing with increasing period. The ranges increase up to 0.5 s for horizontal SAs and up to 0.7 s for vertical ones. The ranges decrease up to $T = 1$ s for horizontal components of SAs while this segment extends up to $T = 2$ s for vertical ones.

Acknowledgements The authors would like to acknowledge International Institute of Earthquake Engineering and Seismology

(IIEES) for its help in providing research documents and Grant Number 659. The authors would like to thank the Building and Housing Research Centre of Iran (BHRC) for providing the accelerographic database.

References

- Abrahamson N, Schneider JF, Stepp JC (1991) Spatial coherency of shear waves from the Lotung. Taiwan large-scale seismic test Structural Safety 10:145–162
- Ambraseys NN, Melville CP (2005) A history of Persian earthquakes. Cambridge university press
- Bastami M (2007) Seismic reliability of power supply system based on probabilistic approach. PhD thesis, Kobe University, Japan
- Bazzurro P, Luco N (2007) Effects of different sources of uncertainty and correlation on earthquake-generated losses. Aust J Civil Eng 4:1–14
- Berberian M, Yeats RS (1999) Patterns of historical earthquake rupture in the Iranian Plateau. Bull Seismol Soc Am 89:120–139
- Bommer JJ, Crowley H (2006) The influence of ground-motion variability in earthquake loss modelling. Bull Earthq Eng 4: 231–248
- Boore DM, Gibbs JF, Joyner WB, Tinsley JC, Ponti DJ (2003) Estimated ground motion from the 1994 Northridge, California, earthquake at the site of the interstate 10 and la Cienega Boulevard bridge collapse, West Los Angeles, California. Bull Seismol Soc Am 93:2737–2751
- Cressie N (1993) Statistics for spatial data: Wiley series in probability and statistics Wiley-Interscience. N Y 15:105–209
- Crowley H, Bommer JJ (2006) Modelling seismic hazard in earthquake loss models with spatially distributed exposure. Bull Earthq Eng 4:249–273
- Crowley H, Bommer JJ, Stafford PJ (2008) Recent developments in the treatment of ground-motion variability in earthquake loss models. J Earthq Eng 12:71–80
- Du W, Wang G (2013) Intra-event spatial correlations for cumulative absolute velocity, arias intensity, and spectral accelerations based on regional site conditions. Bulletin of the Seismological Society of America 103:1117–1129
- Elgamal A, He L (2004) Vertical earthquake ground motion records: an overview. J Earthq Eng 8:663–697
- Esposito S, Iervolino I (2011) PGA and PGV spatial correlation models based on European multievent datasets. Bull Seismol Soc Am 101:2532–2541
- Esposito S, Iervolino I (2012) Spatial correlation of spectral acceleration in European data. Bull Seismol Soc Am 102:2781–2788
- Esposito S, Iervolino I, Manfredi G PGA semi-empirical correlation models based on European data. In: Proceedings of the 14th European Conference on Earthquake Engineering. Ohrid, Macedonia, 2010
- Gianniotis N, Kuehn N, Scherbaum F (2014) Manifold aligned ground motion prediction equations for regional datasets. Comput Geosci 69:72–77
- Goda K, Atkinson GM (2009) Probabilistic characterization of spatially correlated response spectra for earthquakes in Japan. Bull Seismol Soci Am 99:3003–3020
- Goda K, Atkinson GM (2010) Intraevent spatial correlation of ground-motion parameters using SK-net data. Bull Seismol Soci Am 100:3055–3067
- Goda K, Hong H (2008a) Estimation of seismic loss for spatially distributed buildings. Earthquake Spectra 24:889–910
- Goda K, Hong H (2008b) Spatial correlation of peak ground motions and response spectra. Bull Seismol Soci Am 98: 354–365
- Goda K, Hong H (2009) Deaggregation of seismic loss of spatially distributed buildings. Bull Earthq Eng 7:255–272
- Hong H, Zhang Y, Goda K (2009) Effect of spatial correlation on estimated ground-motion prediction equations. Bull Seismol Soci Am 99:928–934
- Jayaram N, Baker JW (2008) Statistical tests of the joint distribution of spectral acceleration values. Bull Seismol Soci Am 98:2231–2243
- Jayaram N, Baker JW (2009) Correlation model for spatially distributed ground-motion intensities. Earthq Eng Struct Dyn 38:1687–1708
- Journel AG, Huijbregts CJ (1978) Mining geostatistics. Academic press,
- Kotha SR, Bindi D, Cotton F (2016) Partially non-ergodic region specific GMPE for Europe and Middle-East. Bull Earthq Eng 14:1245–1263
- Landwehr N, Kuehn NM, Scheffer T, Abrahamson N (2016) A Nonergodic Ground-Motion Model for California with Spatially Varying Coefficients. Bull Seismol Soci Am 106: 2574–2583
- Lee R, Kiremidjian A, Stergiou E Uncertainty and correlation of network components losses for a spatially distributed system. In: proceedings of 13th world conference on earthquake engineering, Vancouver, Canada, August, 2004. pp 1–6
- Lee R, Kiremidjian AS (2007) Uncertainty and correlation for loss assessment of spatially distributed systems. Earthquake Spectra 23:753–770
- Loth C, Baker JW (2013) A spatial cross-correlation model of spectral accelerations at multiple periods. Earthq Eng Struct Dyn 42:397–417
- McVerry GH, Rhoades DA, Smith WD Joint hazard of earthquake shaking at multiple locations. In: Proceedings of 13th world conference on earthquake engineering, Vancouver, Canada, 2004
- Mirzaei N, Mengtan G, Yuntai C (1998) Seismic source regionalization for seismic zoning of Iran: major seismotectonic provinces. J Earthq Predict Res 7:465–495
- Molas G, Anderson R, Seneviratna P, Winkler T Uncertainty of portfolio loss estimates for large earthquakes. In: proceedings of first European conference on earthquake engineering and seismology, Geneva, Switzerland, 2006. pp 3–8
- Papazoglou A, Elnashai A (1996) Analytical and field evidence of the damaging effect of vertical earthquake ground motion. Earthq Eng Struct Dyn 25:1109–1138
- Park J, Bazzurro P, Baker J (2007) Modeling spatial correlation of ground motion intensity measures for regional seismic hazard and portfolio loss estimation Applications of statistics and probability in civil engineering:1–8

- Pavel F, Vacareanu R (2016) Spatial correlation of ground motions from Vrancea (Romania) intermediate-depth earthquakes bulletin of the seismological Society of America
- Sedaghati F, Pezeshk S (2017) Partially nonergodic empirical ground-motion models for predicting horizontal and vertical PGV, PGA, and 5% damped linear acceleration response spectra using data from the Iranian plateau bulletin of the seismological Society of America 107:934–948
- Soghrat M, Ziyaeifar M (2016) Ground motion prediction equations for horizontal and vertical components of acceleration in Northern Iran Journal of Seismology:1–27
- Sokolov V, Wenzel F (2011a) Influence of ground-motion correlation on probabilistic assessments of seismic hazard and loss: sensitivity analysis Bulletin of Earthquake Engineering 9:1339
- Sokolov V, Wenzel F (2011b) Influence of spatial correlation of strong ground motion on uncertainty in earthquake loss estimation. Earthq Eng Struct Dyn 40:993–1009
- Sokolov V, Wenzel F (2013) Further analysis of the influence of site conditions and earthquake magnitude on ground-motion within-earthquake correlation: analysis of PGA and PGV data from the K-NET and the KiK-net (Japan) networks. Bull Earthq Eng 11:1909–1926
- Sokolov V, Wenzel F, Wen K-L, Jean W-Y (2012) On the influence of site conditions and earthquake magnitude on ground-motion within-earthquake correlation: analysis of PGA data from TSMIP (Taiwan) network Bulletin of Earthquake Engineering:1–29
- Stafford PJ (2014) Crossed and nested mixed-effects approaches for enhanced model development and removal of the ergodic assumption in empirical ground-motion models. Bull Seismol Soci Am 104:702–719
- Wang G, Du W (2013) Spatial cross-correlation models for vector intensity measures (PGA, Ia, PGV, and SAs) considering regional site conditions bulletin of the seismological Society of America
- Wang M, Takada T (2005) Macrospatial correlation model of seismic ground motions. Earthq Spectra 21:1137–1156
- Wesson RL, Perkins DM (2001) Spatial correlation of probabilistic earthquake ground motion and loss. Bull Seismol Soci Am 91:1498–1515
- Zahrai S, Heidarzadeh M (2007) Destructive effects of the 2003 bam earthquake on structures. Asian J civil Eng (build Hous) 8:329–342
- Zerva A, Zervas V (2002) Spatial variation of seismic ground motions: an overview. Appl Mech Revi 55:271–297